The influence of strong tides on the formation of Amundsen Sea Polynya

Mengting Zhuo[1,2], Song Hu[3], Yu Hong[1,2], and Yan Du[1,2]

[1]State Key Laboratory of Tropical Oceanography, South China Sea Institute of Oceanology, Chinese Academy of Sciences, Guangzhou, China.

[2]University of Chinese Academy of Sciences, Beijing, China.

[3]College of Marine Science, Shanghai Ocean University, Shanghai, China.

Corresponding author: Yan Du (duyan@scsio.ac.cn)

Key Points:

- The geographical location and shape of the Amundsen Sea Polynya were closely related to the underwater ridge (Bear Ridge).
- The atmosphere-dominated polynya event was caused by significant cross-ridge winds and surface net solar radiations.
- Four of the five largest polynya events occurred mainly during spring tides, which were tide-dominated events affected by the strengthening vertical mixing of seawater.

Abstract

Polynyas play an important role in climate change with an efficient exchange of heat and matter between the atmosphere and the ocean in polar regions. This study investigated the influence of strong tides and atmospheric forcing on the Amundsen Sea Polynya, especially focusing on large-area polynya events from 2002 to 2020. We found that the geographical locations of the polynyas are closely related to the underwater ridge, where tidal currents are relatively strong. More importantly, strong cross-ridge winds are the "triggers" above the sea surface for the initial formation of the Amundsen Sea Polynya, while strong tides under the sea surface tend to create large-area polynya. Four of the five largest polynya events occurred mainly during spring tides. Only the 2016 event occurred during the normal tide period, which was atmosphere-dominated. Strong tides significantly affect the evolution of polynyas by strengthening the vertical mixing of seawater. Given that ocean in Antarctica might become warmer, tidal mixing might enhance the mixing in the future climate.

Plain Language Summary

The polynya is a water area that does not freeze or has only thin ice when it reaches freezing conditions in winter. As a window between ocean and atmosphere, polynyas play an important role in climate change. The polynya is the result of the interaction of atmosphere, sea ice and ocean. This study focused on the major polynya events and the initial formation of the polynya using the sea ice concentration (SIC) data of the University of Bremen based on AMSR-E/2. We found that the geographical location of the polynya was closely related to the topography. The polynya extended to the open ocean along the terrain of the Bear Ridge. The formation of the Amundsen Sea Polynya was affected by the atmosphere and the ocean. Winds was the "triggers" for the formation of the Amundsen Sea Polynya. The wind field on the days when the Polynya splits was dominated by northwest and southeast winds (ESE, E, and WNW), which were cross-

ridge (Bear Ridge). The surface net solar radiations also played an important role in the area of the Amundsen Sea Polynya. The area of the polynya was large during spring tides related to the local spring tides, that is, the area was large during spring tides. Strong tides significantly affect the evolution of polynyas by strengthening the vertical mixing of seawater. Ocean in Antarctica might become warmer because of the global warming, tidal mixing may be more important for the future climate.

1 Introduction

As one of Antarctica's fastest melting marginal seas, the Amundsen Sea is closely related to the global climate and has become a hot area of geoscience (Kim et al., 2021). The Amundsen Sea is located in West Antarctica (Figure 1), south of 71°S (100°W~135°W), on its east Thurston Island, and its west Cape Dart, the cape of Siple Island, which is part of the South Pacific Ocean connecting the Ross Sea and the Bellinsgauzen Sea. The Amundsen Sea is characterized by deep troughs extending to the continental shelf fault (Jacobs et al., 2012). The direction of the extent of the troughs is north-northeast, and the troughs gradually narrow towards the Pine Island Trough with Bear Ridge on its west (Hogan et al., 2020).

The melting of ice in the Amundsen Sea has been accelerating due to the rising global temperatures (Nakayama et al., 2021). The mass loss rate of Antarctic glaciers gradually increased from 40±9 Gt/y in 1979-1990 to 252±26 Gt/y in 2009-2017 (Rignot et al., 2019). Among them, the loss of glacier mass in West Antarctica took place mainly in the Amundsen Sea (Hogan et al., 2020; Rignot et al., 2019). Meanwhile, the mass loss rate of the Getz Ice Shelf in the Amundsen Sea area was 16.5 Gt/y in 2017, three times higher than that in 1979-2003 (Rignot et al., 2019). In addition, the Amundsen Sea played an important role in the mass balance of West Antarctica glaciers and the rise in sea levels (Shepherd et al., 2019; Shepherd & Wingham, 2007). Thus, as the monitor of the Antarctic and global climate change, how the polynya in the Amundsen Sea has changed in these years deserves our attention.

The Amundsen Sea Polynya is the main large polynya in Antarctica. A good number of studies focused on its high primary productivity rather than its formation (Arrigo et al., 2012; Lee et al., 2016; Thuróczy et al., 2012). A recent study by Macdonald et al. (Macdonald et al., 2021) focused on the physical process of its formation. They found a concurrence of the highest polynya areas in 2020 after April and the highest spikes in wind speed. However, as a window connecting the atmosphere, sea ice, and ocean, the Amundsen Sea Polynya can be modified by multiple factors.

Additionally, many studies have shown that polynyas are closely related to tides. In 1984 it was proposed that tides play a major role in the polynya in the western Canadian Arctic (Melling et al., 1984). Afterward, a study of the polynya in the Kashevarov Bank found in the Okhotsk Sea showed that the resonance of the O_1 and K_1 harmonic constituents increased vertical heat flux, which significantly affected the formation and change of the polynya (Martin, 2004). The polynya showed an obvious two-week cycle in the winter of 2000-2001 (Martin, 2004). Tides also impact the North Water Polynya, resulting in a 12-hour periodic change in the polynya (Vincent & Marsden, 2008). The above studies mainly focused on the northern hemisphere (Hannah et al., 2009). Possibly due to the remote location and great attention on the ice shelves, so far as we know, there are yet no studies focusing on the impact of tides on the Amundsen Sea Polynya. Previous studies have shown that tides can enhance the melting of the Amundsen Sea ice shelves by increasing the exchange between ice and ocean (Jourdain et al., 2019). However, the evolution of the Amundsen Sea Polynya related to tides attracts our attention after a detailed

examination.

Owing to the development of passive microwave remote sensing, AMSR-E data provided an opportunity to study the evolution of polynyas in much better detail than before. In this study, we used the sea ice concentration (SIC) data of the University of Bremen based on AMSR-E/2. We focused on the major polynya events and paid attention to the initial stages of the Polynya formation and the maximum area of each polynya. Furthermore, we comprehensively considered the oceanic factors (topography, tides) and atmospheric factors (wind, surface net solar radiation) of the Amundsen Sea, allowing us to analyze the mechanism of the large-area events from 2002 to 2020.

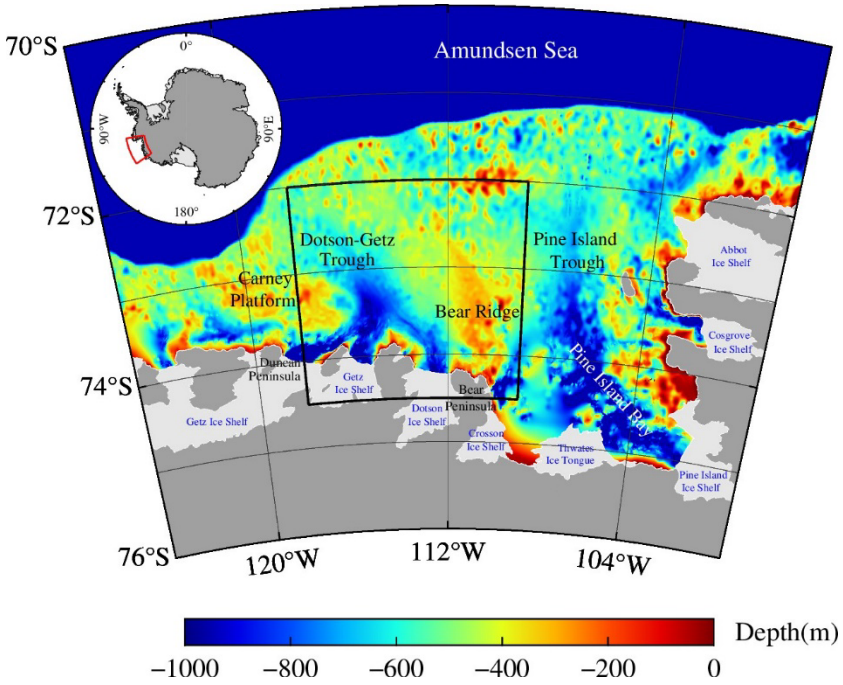

Figure 1. The topography of the Amundsen Sea, Antarctica. The black line is the main area where polynyas occurred.

2 Data and methods

2.1 Data

The SRTM15+ V2.1 global bathymetry and topography dataset (Tozer et al., 2019) from Open Topograph (Wessel et al., 2019) was used for the bathymetry of the study region. The dataset used was the latest iteration of the SRTM+ digital elevation model (DEM) with a grid of 15 arc seconds.

The sea ice concentration dataset, version 5.4 (Spreen et al., 2008) from the University of Bremen, Institute of Environmental Physics (IUP) was used. The data was retrieved with the ARTIST Sea Ice (ASI) algorithm (Spreen et al., 2008) based on AMSR-E (Advanced Microwave Scanning Radiometer for EOS, June 1st, 2002—October 4th, 2011) and AMSR2 (Advanced Microwave Scanning Radiometer 2, July 2nd, 2012—today). The data in HDF4 format with a spatial resolution of 3.125 km×3.125 km includes a daily time series of sea ice concentrations over the period 2002—2020 for the south polar regions, but the data from October 5th, 2011, to July 1st, 2012, and other individual times were missing.

Wind and surface net solar radiation data were all obtained from the European Centre for Medium-Range Weather Forecasts (ECMWF) ERA5 dataset. The dataset was obtained from the Copernicus Climate Change Service (C3S) at ECMWF. We combined the eastward and northward components of the 10m wind to give the speed and direction of the horizontal 10m wind. These data with a spatial resolution of 0.25°×0.25° have a temporal resolution of 1 day. If the vertical heat flux (surface net solar radiation) is positive, the heat transfer direction is downward.

TPXO tide models (Egbert & Erofeeva, 2002) developed by the Oregon State University (OSU) were used to predict the tide level. TPXO9-atlas models have a spatial resolution of 1/30° globally provided by National Computational Infrastructure (NCI). The models include 8 primary (O_1, K_1, S_2, P_1, M_2, N_2, Q_1, and K_2) and 4 non-linear ($2N_2$, M_4, MS_4, and MN_4) harmonic constituents. A position of 112°W and 73°S was chosen to represent the study region, and a tide level from 2002 to 2020 was obtained.

2.2 Methods

2.2.1 Study time

The timing of freezing and melting of sea ice in the Amundsen Sea differs from that in other regions of Antarctica, which have certain regional characteristics (Stammerjohn et al., 2012). The monthly sea ice concentration in the Amundsen Sea (125W~99W, 76S~70S) from 2002 to 2020 was 33.29%-95.73% (Figure 2). On average, sea ice concentration was lowest in February and highest in July. Interannual sea ice variation was greatest in March, the early stages of glaciation, with a standard deviation of 19.22%. Sea ice concentration was relatively stable in July, which was the highest value of sea ice concentration in those years, with a standard deviation of 0.84%. Because the polyna is an area that is not covered by sea ice when it reaches the freezing condition. June to October was selected as the study period for polynyas, with high sea ice concentration and low interannual sea ice variation.

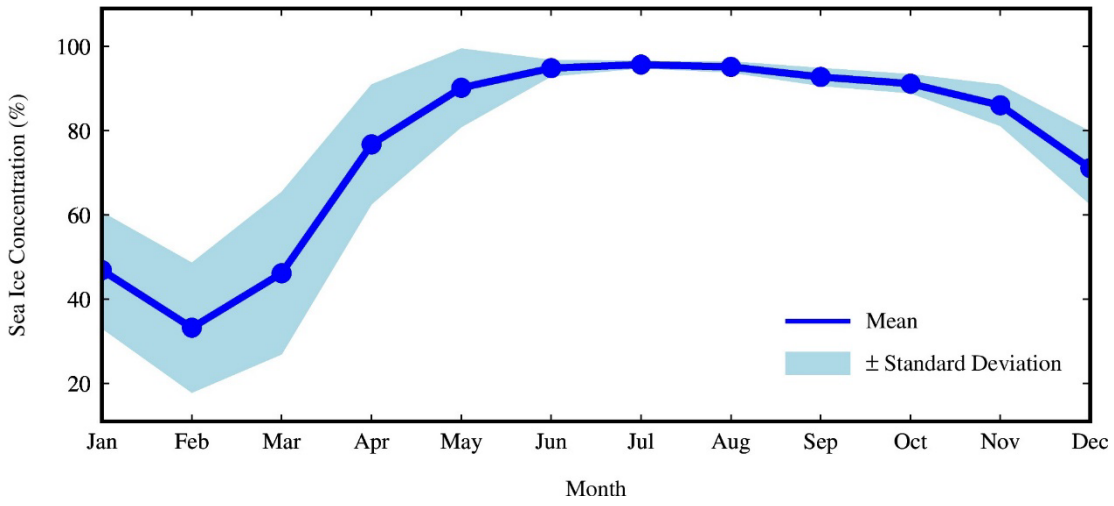

Figure 2. The monthly sea ice concentration in the Amundsen Sea (125°W~99°W, 76°S~70°S) from 2002 to 2020. The blue line is the mean sea ice concentration of each month, and the shaded blue is the standard deviation of the mean sea ice concentration for each month in 19 years.

2.2.2 Study site

Polynyas can generally be distinguished by sea ice concentration and sea ice thickness (Massom et al., 1998; Preusser et al., 2019). In this study, polynyas are distinguished by the sea ice concentration, and the 75% sea ice concentration value is taken as the threshold for judging the polynya (Massom et al., 1998). It is considered that the area with less than 75% sea ice concentration is the polynya area, and the area with more than 75% sea ice concentration is the sea ice area. Thus, the occurrence frequency of the Polynya in the Amundsen Sea from 2002 to 2020 was evaluated (Zhang et al., 2021). The main area of polynya in the Amundsen Sea was assumed to be the area with a high occurrence frequency (Figure 3). The Amundsen Sea is normally covered by sea ice from June to October. However, along the Bear Ridge and the east coast of Pine Island Bay, one large polynya and a series of coastal polynyas always regularly occurred during this period. Therefore, waters of Amundsen Sea Polynya (118W~109W, 74.5S~72S) with high occurrence frequency were framed with solid red lines, which was selected as the main study area (Figure 3). The Amundsen Sea Polynya is a perennial water area surrounded by high sea ice. Most of the time, the shape of polynya was an arc, extending northward from the coast of Bear Ridge with the tip facing west.

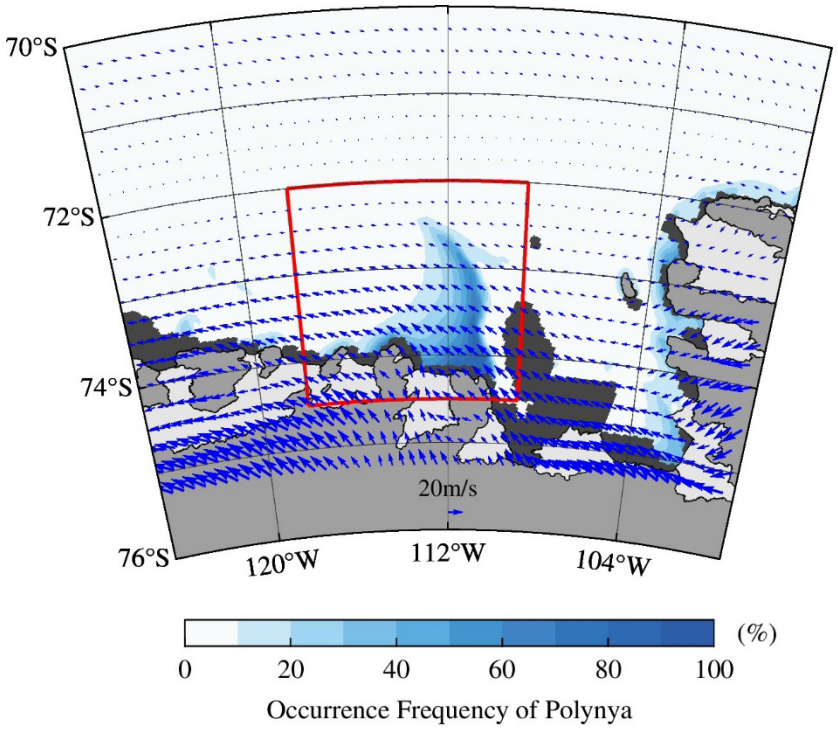

Figure 3. The occurrence frequency of polynya and mean wind field distribution in the Amundsen Sea over the period 2002-2020. The solid red lines is the main study area.

2.2.3 Calculation of polynya area

The sea ice concentration data with a spatial resolution of 3.125 km×3.125 km was used in this study. According to each grid area, the area of the Amundsen Sea Polynya was calculated by water area integral:

$$S = \int (1 - C) ds \quad (1)$$

Where C is the sea ice concentration, s is the single grid area (with 75% sea ice concentration value as the threshold), and S is the area of the polynya.

3 Results

3.1 Impact of cross-ridge wind on triggering polynya

The mean wind speed in the Amundsen Sea area (125°W~99°W, 76°S~70°S) from June to October 2002 to 2020 was 8.05 m/s. As seen in Figure 3, the mean wind field had a good relationship with the occurrence frequency of Amundsen Sea Polynya. The wind speed along the coast of the study area (red frame) was large, and the overall wind direction was offshore, south-easterly. It was a cross-ridge wind that roughly coincided with the splitting direction of the Polynya and was perpendicular to the direction of the Polynya extension.

The area of the Polynya is generally 10-10^5 km^2 (Morales Maqueda et al., 2004), and the mean area of the Amundsen Sea Polynya in winter was 4.53×10^3 km^2. Results showed that when the area of the Amundsen Sea Polynya was less than 400 km^2, this identified a situation of complete ice cover in the study area. If the area of the Amundsen Sea Polynya exceeds 400 km^2 one day and this day is the day after a completely freezing day, this day is the day when the Polynya splits and the first day of a polynya event. The period from this day to the next complete ice cover is considered as a complete Amundsen Sea Polynya event. For example, in 2018, the study area was completely covered by sea ice from August 2nd to 4th and September 22nd, the area of the Polynya exceeded 400 km^2 from August 5th to 21st. It was considered that the period from August 5th to September 22nd was a complete Amundsen Sea Polynya event. It was considered that August 4th is the day before the Polynya splits, and August 5th is the day when the Polynya splits. The Amundsen Sea Polynya happened in most cases from June to October every year, and was completely covered by sea ice for only 163 days in 19 years.

Studies have shown that some large polynya events may be caused by strong wind events (Macdonald et al., 2021). The change of the Amundsen Sea Polynya affected by the wind field occurred mainly on the synoptic scale in terms of time. Using the Beaufort scale (Penwarden, 1973), the wind field in the study area was dominated by southeast offshore winds all year round (Figure 4a). ESE was the main wind direction, accounting for 16.19 %. In contrast, the proportion of westerly wind direction was relatively low. Figures 4b and 4c show the distribution of the mean wind speed and direction in the study area from January to May in summer and June to October in winter, respectively. The relative proportion of each wind direction in summer and winter was consistent with the distribution of wind direction throughout the year, mainly dominated by southeast winds (ESE and SE). The proportion of higher wind speeds in winter was higher than in summer. The proportion of higher wind forces of 7 and above (>13.9 m/s) was only 4.86 % in summer, while it accounted for 9.74 % in winter.

On days with complete frost, before and after the formation of the Polynya, the wind field

distribution in the study area was very different from that in normal times (Figure 4d-f). On days with complete frost and the days before the Polynya split (Figure 4d, e), the main wind direction was Northwest (W and WNW). However, the main wind directions, which were Southeast (ESE and E) and Northwest (W and WNW) in the study area, were cross-ridge on the days when the Polynya splits (Figure 4f). The proportion distribution of the individual wind directions was completely different from when it was frozen and the days before the Polynya splits. Compared to the long-term mean wind field, the westerly wind direction (WNW and W) had a large proportion on the day when the Polynya splits, followed by the largest proportions of the ESE and E directions with about 8.26% and 6.07%, respectively. In particular, on the day when the Polynya splits, the wind speed was great. The proportion of higher wind speeds of force 7 and above was high at 13.09%. The wind direction was generally dominated by the northwest coastal winds when it was fully frozen and the days before the Polynya splits. Therefore, the northwest coastal winds were conducive to the Polynya area being completely covered by sea ice. The strong cross-ridge wind in the study area could easily blow away the sea ice, leading to the formation of the Polynya.

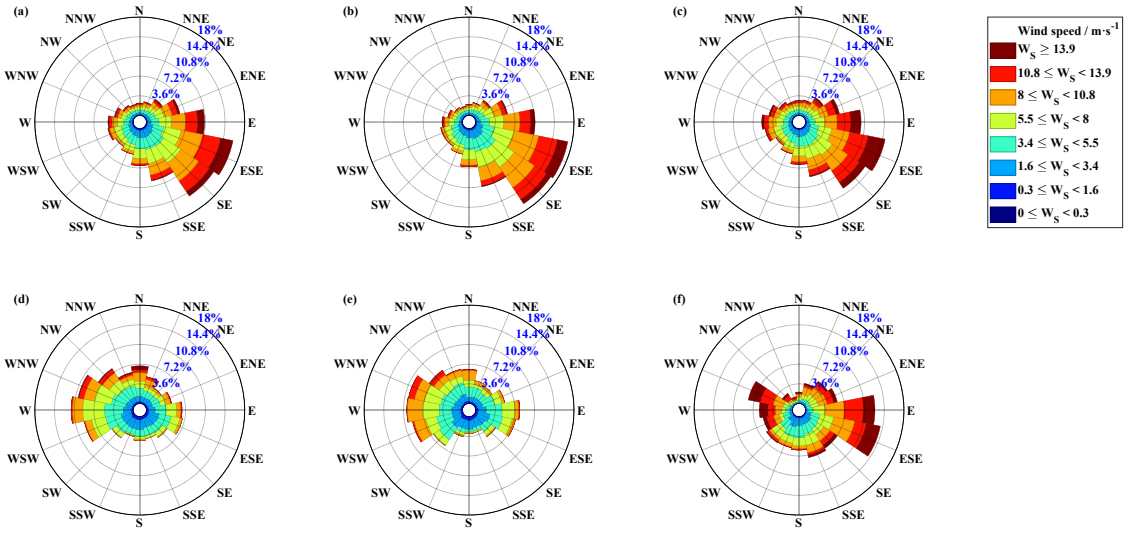

Figure 4. The percentage distributions of wind speed and direction in different times **a.** all days, **b.** the days from January to May in summer, **c.** the days from June to October in winter, **d.** the completely freezing days, **e.** the days before the Polynya splits and **f.** the days when the Polynya splits over the period 2002-2020.olid red lines is the main study area.

3.2 Impacts of the ridge on the Polynya

The continental shelf narrows from east to west and the depth north of it exceeds 1000 m (Figure 5). Along the coast, there are two deep inland shelf troughs with the longitude of about 115°W and 106°W and a depth of more than 1000 m. There are two areas with shallow depth to the west and in the middle of the two troughs. The Carney platform near 119°W to the west has relatively high terrain and a depth of about 100 m to 200 m. The Bear Ridge 111°W to the east is also relatively shallow and extends west toward the open ocean.

When the area of the Amundsen Sea Polynya was small, regardless of the small water area

to the north of 72°S, we could observe that the Polynya matched perfectly with the bathymetry, mainly distributed in an arc from the coast to the outside. Figure 5 shows the situation of all the days during the initial period of the Polynya splitting, when the Polynya was small in the Amundsen Sea from June to October 2020. The Polynya started from the Bear Peninsula near 111°W, extended to the open ocean in the north along the topography of the Bear Ridge, and the northernmost tip of it faced west. Furthermore, there was also an occasional polynya in the Amundsen Sea in 2020, extending along the topography from the Duncan Peninsula near 119°W to the edge of the western continental shelf along the Carney Platform. The shape of the Polynya was also similar to that of the Amundsen Sea Polynya. They were both shaped as an arc, with the northernmost tip facing west. It could be seen that the topography plays an important role in the formation of the Polynya and affects its location and shape.

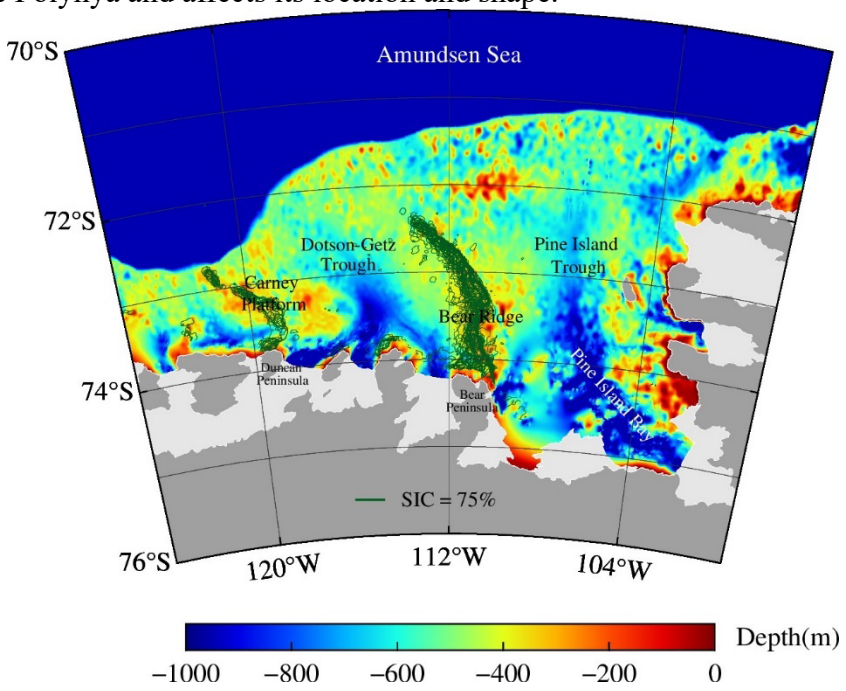

Figure 5. The topography and the distribution of the Polynya (green lines) during the initial splitting period of the Amundsen Sea Polynya from June to October 2020.

3.3 Large-area polynya events

3.3.1 Tides

Figure 1. Amplitude and phase lag of harmonic constituents.

harmonic constituent	amplitude/ m	phase lag/°	harmonic constituent	amplitude/ m	phase lag/°
O_1	0.244	99.9	Q_1	0.054	89.7
K_1	0.174	87.1	K_2	0.033	163
S_2	0.134	160.7	$2N_2$	0.011	176
P_1	0.107	118.4	M_4	0.003	83.2
M_2	0.063	-107.5	MS_4	0	166.8
N_2	0.061	-160	MN_4	0	39.6

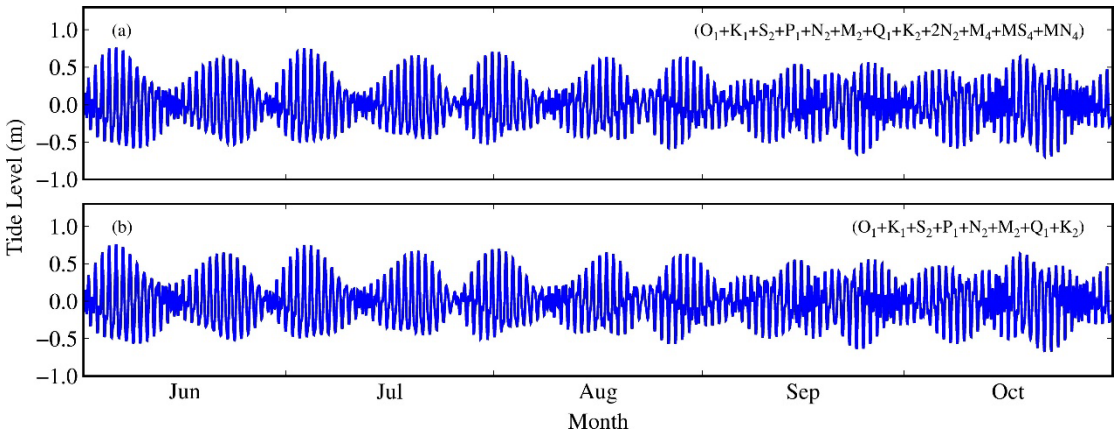

Figure 6. The time series of tide level in the study site from June to October in 2020. **a.** including 8 primary (O_1, K_1, S_2, P_1, M_2, N_2, Q_1 and K_2) and 4 non-linear ($2N_2$, M_4, MS_4 and MN_4) harmonic constituents, **b.** only including 8 primary harmonic constituents.

The position (112°W, 73°S) was chosen to investigate the tides in the study region. Taking the tide level from June to October in 2020 as an example, the amplitude of O_1, K_1, S_2, P_1 primary harmonic constituents were higher (above 0.1m) than in other months. There were four extremely low non-linear ($2N_2$, M_4, MS_4, and MN_4) harmonic constituents, and we ignored them by comparing Figure 6a and Figure 6b. There were two high and two low water in this site in a day, which belongs to the irregular semidiurnal tide. The tides from June to August in the Amundsen Sea area generally alternated between a 16-day cycle and a 12-day cycle. Based on the spring tide from June to August, there were still some spring tides with relatively low tide levels in September and October. The frequency of spring tides in these two months was relatively high.

We presented the tides, including 2 primary (O_1 and K_1) harmonic constituents in Figure 7a. In Figure 7b, we considered P_1 primary harmonic constituents based on Figure 7a. By comparing them, it could be considered that spring tides changed because of P_1. Unlike Figure 7a, there were regular tides in Figure 7a with a tide level of 0.43m at high water hours. The tide level of spring tides changed. Thus, the tide level of spring tides reached the lowest value in early September, at 0.33m. We presented the tides, including all primary harmonic constituents (O_1, K_1, S_2, P_1, M_2, N_2, Q_1, and K_2) in Figure 7f, but did not consider P_1 primary harmonic constituents in Figure 7d. We can also draw the conclusion that P_1 played an important role in lowering the tide level of spring tides but raising the tide level of neap tides in early September.

Similarly, we considered the role of S_2 in the site by comparing Figure 7a with Figure 7c and comparing Figure 7e with Figure 7f. It was observed that S_2 made spring tides higher, which was most obvious in July. It also increased the original neap tides and became part of some low spring tides. There were two similar level spring tides in October because of S_2, so the spring tides' frequency increased. Thus, by detailed examination, we considered that P_1 and S_2 were two of the most important harmonic constituents contributing to the irregular pattern of tides in the region.

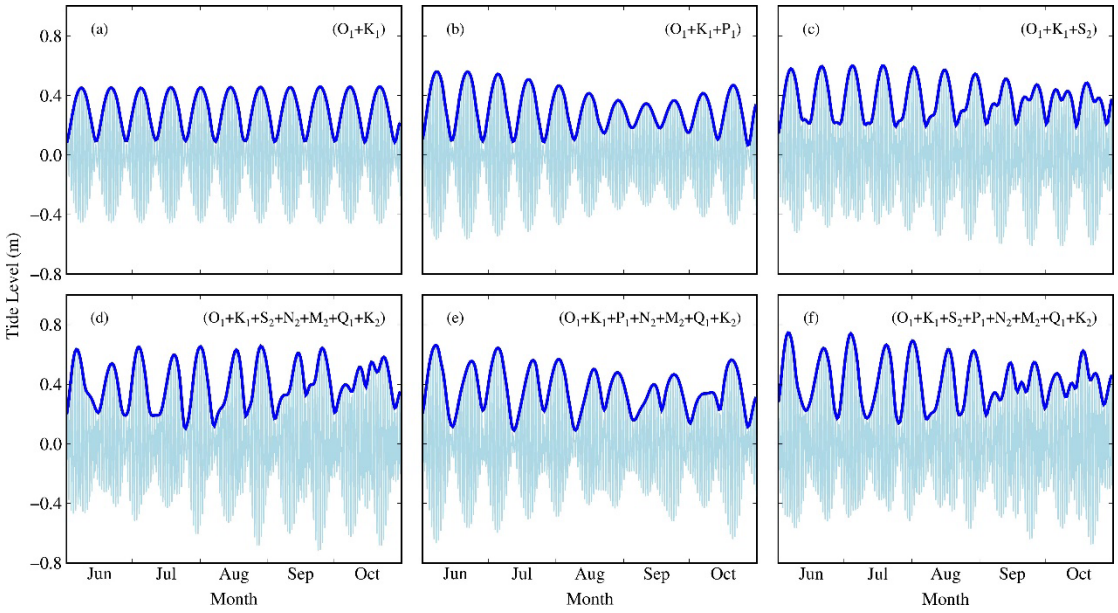

Figure 7. Tide level was most significantly affected by P_1 and S_2 primary harmonic constituents in the study site from June to October 2020. In this part, only the 8 primary harmonic constituents were considered. **a.** the tides including 2 primaries (O_1 and K_1) harmonic constituents, **b.** on the basis of **a.**, consider P_1 primary harmonic constituents, **c.** on the basis of **a.**, consider S_2 primary harmonic constituents, **f.** including all primary (O_1, K_1, S_2, P_1, M_2, N_2, Q_1 and K_2) harmonic constituents, **d.** on the basis of **f.**, did not consider P_1 primary harmonic constituents, **e.** on the basis of **f.**, did not consider S_2 primary harmonic constituents.

3.3.2 Impacts of tides on polynya

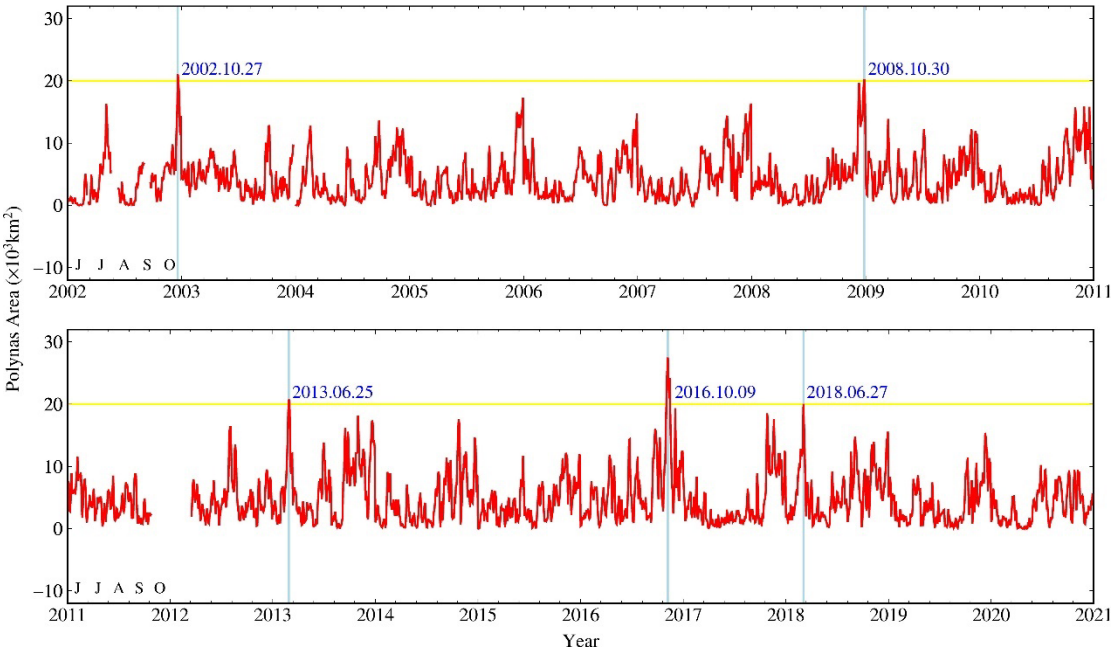

Figure 8. The time series of the Polynya area from June to October over the period 2002-2020. The yellow line indicates the value of $20\times10^3km^2$ to find the five largest-area polynya events. The dates of the five largest-area events are marked with blue lines.

According to the time series of the Amundsen Sea Polynya area (Figure 8), five large-area polynya events with an area of more than $20\times10^3km^2$ were selected to analyze the environmental characteristics before their occurrence. The study area was represented by the position (112°W, 73°S), and the TPXO9-atlas models, including 8 primaries (O_1, K_1, S_2, P_1, M_2, N_2, Q_1, and K_2) and 4 non-linear ($2N_2$, M_4, MS_4, and MN_4) harmonic constituents were used for tide prediction. It could be seen from the prediction that the tide in the study area belonged to an irregular semidiurnal tide. We found that four of the five events (events B-F) with the largest area of the Polynya occurred within 3 days after the spring tide (Table 2), which may be a tide-dominated polynya. Therefore, it suggested that the tides may be a factor in the change of the Amundsen Sea Polynya. Unlike regular tides patterns in similar studies on the northern hemisphere (Hannah et al., 2009; Martin, 2004; Melling et al., 1984; Vincent & Marsden, 2008), the irregular tides pattern caused by P_1 and S_2 makes the study on the link between tides and polynyas more complex.

Figure 2. Analysis of the characteristics of large polynya events.

Events	Maximum area（$\times10^3km^2$）	Maximum area occurrence time	Time of last spring tide	Days from spring tide	Mean surface net solar radiation in the first five days（$\times10^5J\cdot m^{-2}$）
A	27.50	2016.10.09	2016.10.04	5	1.39
B	21.08	2002.10.27	2002.10.24	3	2.95
C	20.74	2013.06.25	2013.06.22	3	0
D	20.29	2008.10.30	2008.10.30	0	3.41
E	20.04	2018.06.27	2018.06.26	1	0

It can be seen from Table 2 that the mean surface net solar radiation five days before the Polynya events was very different. This was because they occurred in different months, in June and October, respectively. The surface net solar radiation in June was $0\,J\cdot m^{-2}$ (Figure 8), and the radiation in October was large. The radiation in the first five days of events A, B and D in October exceeded the mean surface net solar radiation in the study area (Table 2). Event A was the largest polynya event in 19 years. In this event, the date when the area of the Polynya exceeded $20\times10^3km^2$ was October 7th-12nd. Although the largest area of this event did not occur during the spring tide, the area also exceeded $20\times10^3km^2$ on the third day after spring tide, which provided a basis for the occurrence of the largest area. Moreover, the mean radiation in the first five days was large, and it was characterized by the strong cross-ridge wind from October 2nd to October 9th. This event did not disappear until October 17th. Therefore, we consider that this event was an atmosphere-dominated event, which was caused by unusually significant cross-ridge wind and surface net solar radiation.

3.4 Impact of surface net solar radiation on polynya

The net surface solar radiation in the study area from June 1st to August 23rd throughout the

19 years was $0\,J \cdot m^{-2}$(Figure 9). Radiation gradually increased from the end of August every year; In addition, radiation peaked in winter at the end of October. The mean net insolation at the surface from September to October 2002 to 2020 in the study area was$1.37 \times 10^5 J \cdot m^{-2}$. Compared to the time series of the Amundsen Sea Polynya, it can be seen that late October, with large surface net insolation, was generally the time when the area of the Polynya was the largest. The Polynya area was also large in the three years of large-scale net solar radiation in 19 years (2002, 2008, and 2017). It is worth noting that on October 31st, 2008, net solar radiation at the surface reached its highest level making it the fourth largest polynya in 19 years with a total area of $5.14 \times 10^5 J \cdot m^{-2}$. In addition, on October 9th, 2016, the area of the Polynya reached 2.75×10^4km^2, the maximum in 19 years. The surface net solar radiation in October of this year was the second largest value in 19 years, only after 2008. There is an apparent corresponding relationship between the surface net solar radiation and the area of the Polynya. The area with large surface net solar radiation in the ocean hinders the generation of sea ice, which is conducive to the formation and development of polynya. When the polynya is large, it can absorb more solar radiation due to the lack of sea ice coverage with higher albedo. The surface net solar radiation of the ocean is thus increased, which may make the polynya have a larger area. Therefore, because of the positive feedback relationship between sea ice and solar radiation, the surface net solar radiation is of great significance for the polynya.

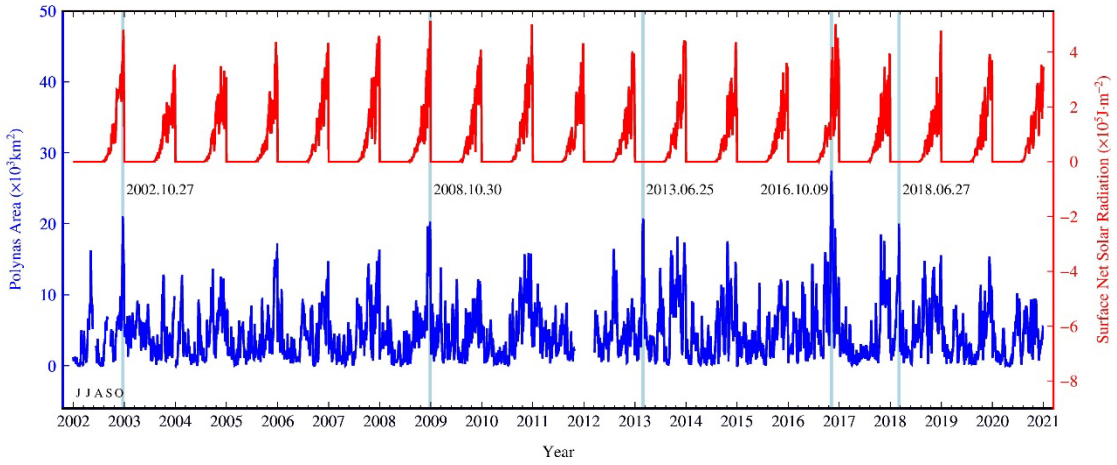

Figure 9. The time series of the Polynya area and the surface net solar radiation from June to October 2002-2020. The blue line indicates the Polynya area and the red line is the surface net solar radiation in 19 years (the positive values in the radiation indicate that the heat transfer direction is downward).

4 Discussion

4.1 Impacts of oceanic factors on polynya

As a key channel for the interaction between the atmosphere, ice, and ocean, the Amundsen Sea Polynya offers a unique perspective on climate change. With the development of field observation and marine satellite remote sensing, more and more ocean data are available for studying polynya. The remote Amundsen Sea has also received increased attention (Jacobs et al., 2012) and topographical data in the vicinity of the Amundsen Sea has been continuously updated (Hogan et al., 2020; Nitsche et al., 2007), laying the foundations for an oceanographic

exploration of the Amundsen Sea. It was found that Amundsen Sea Polynya existed in most cases from June to October every year, but was completely frozen for only 163 days in 19 years. The mean area of the Amundsen Sea Polynya was 4.53×10^3 km^2 in winter, reaching the maximum area of 2.75×10^4 km^2 on October 9th, 2016. In general, the area of the Polynya reached a large value at the end of winter (October). Arrigo et al. (Arrigo et al., 2012) showed that the mean area of the Amundsen Sea Polynya was about 2.7×10^4 km^2 in spring and summer, and the area decreased to less than 10000 km^2 by the end of March. This was different from the calculation in this study, which may be due to the different selection of study area and study period.

Ocean changes play an important role in sea ice and polynya in the Antarctic (Hellmer et al., 2012) and can affect the stability of the ice shelves in the West Antarctic (Jacobs et al., 2012). It was an important pillar in maintaining the existence of polynya (Parkinson, 1983). Previous studies have shown that the distribution of the Weddell Sea Polynya and its nearby vertical heat flux was affected by topography (Maud Rise) (Bagriantsev et al., 1989; Gordon & Huber, 1990). And there have been models explaining the reasons for the formation and maintenance of the Weddell Sea Polynya, which could be due to the increase in seawater mixing due to topography (Ou, 1991). Similarly, the Amundsen Sea Polynya matched well with the topography (the Bear Ridge) in the initial stage of the formation of the Amundsen Sea Polynya, which was mainly distributed in an arc from the coast to the open ocean.

As a periodic ocean phenomenon, tides also significantly affect the changes in regional polynyas. Compared to the northern hemisphere, the Antarctic is more difficult to access. We found that the Amundsen Sea tides are influenced by the harmonic constituents S_2 and P_1. Although the mean cycle of the spring tide was 14 days, it was very erratic, making the corresponding comparison between spring tide and polynya not so straightforward. Unlike others, the change in polynyas due to the action of tides had a relatively clear cycle (Martin, 2004; Vincent & Marsden, 2008). However, it is worth noting that there were four major polynya events at the Amundsen Sea, all of which occurred within 3 days of the spring tide. The tides may play some role in the formation of the Amundsen Sea Polynya. In addition, larger waves during spring tide may also be one of the reasons for polynya areas, which need to be further studied.

Similar to recent studies on ice shelf melting, they found that tides are closely related to the melting of Antarctic ice shelves (Hausmann et al., 2020; Huot et al., 2021; Jourdain et al., 2019; Richter et al., 2022). Tides increase the vertical mixing of seawater, so the kinetic energy of the current increases in contact with ice shelves (Hausmann et al., 2020). Tides thus contribute greatly to the exchange of heat and salt between the ice and the ocean (Richter et al., 2022). Tides have been shown to enhance ice shelf melting in the Amundsen Sea by increasing heat flux transfer between sea ice and the ocean (Jourdain et al., 2019; Richter et al., 2022). Similarly, in the D'Urville Sea, it has been found that at low tide, ice shelf ground melt increases (Huot et al., 2021). But we do not currently know the specific effect of the tides on the polynyas. In the follow-up work, it is necessary to strengthen the study of the relationship between local tides and polynyas. It is particularly important to make clear the mechanism of tides on the Amundsen Sea Polynya.

4.2 Impacts of atmospheric factors on polynya

Atmospheric action is also very important for polynya formation, and the wind is the key factor for polynya formation (Parkinson, 1983). Coastal polynya is the result of sea ice advection caused by wind. The size of the polynya depends on the duration and intensity of the wind

(Comiso et al., 2011). There was a good correspondence between the mean wind field in the study area and the occurrence frequency of the Amundsen Sea Polynya. This was consistent with the results of MacDonald et al. (Macdonald et al., 2021) on the spatial distribution of the mean wind field in the Amundsen Sea. And they found that the daily mean wind speed had a weak positive correlation with the area of the Polynya in the Amundsen Sea. Furthermore, showing the wind field with wind roses, we add that the Amundsen Sea Polynya was directly related to the cross-ridge wind in the site. The wind speed along the coast was large, and the direction was cross-ridge, which was roughly consistent with the splitting direction of the Polynya and perpendicular to the Amundsen Sea Polynya extent. Similarly, studies near the Halley research station also showed that the formation and closure of polynyas were highly related to winds (Markus & Burns, 1993). The change of the Amundsen Sea Polynya affected by the wind field is mainly the synoptic scale in terms of time (Arrigo et al., 2012). Before and after the formation of the Polynya, the wind field distribution in the study area was very different from that in normal times. On the day when the Polynya splits, the main wind direction in the study area was southeast (ESE and E) and northwest (W and WNW). The northwest and southeast winds were cross-ridge, perpendicular to the terrain of Bear Ridge, which easily blew away the sea ice, resulting in the formation of the Polynya.

Solar radiation enters the ocean surface, melting the sea ice and leading to the generation of polynyas (Morales Maqueda et al., 2004). There was an obvious relationship between the surface net solar radiation and the area of the Polynya. The area of the Polynya during 19 years was greater for three years (2002, 2008 and 2017) associated with large surface net solar radiations. The area of the Polynya reached its maximum value on October 9th, 2016. The surface net solar radiation in October of that year was the second largest value in 19 years. Tides were not the cause of the largest polynya events on October 9th, 2016. The area of the Polynya will increase with the increase of the surface net solar radiation, due to the positive feedback relationship between the polynya and the surface net solar radiation. We considered that this event was an atmosphere-dominated event, which was caused by a large surface net solar radiation and a special air-sea interaction condition.

The Amundsen Sea Polynya reached the maximum area on October 9th, 2016. This year has been greatly studied and could be a special year that could be affected by the significant strong El Niño phenomenon in 2015-2016 (Meehl et al., 2019). From September to October 2016, the Antarctic experienced a sharp decline in sea ice cover (Meehl et al., 2019). The sea ice melting time unusually advanced in 2016. The time when the sea ice range in Antarctica reached its maximum advanced from September to August (Schlosser et al., 2018). MacDonald et al. (Macdonald et al., 2021) also showed that there were records of low sea ice conditions from 2016 to 2017, which significantly affected the Amundsen Sea Polynya area. Thus, we think that the effect of the atmosphere was more significant than that of tides in this special year, so one of the large polynya events did not occur during spring tides. However, the remaining four large polynya events occurred during spring tides, suggesting that tides were more common factors.

Many studies have shown that the sea water in the west Antarctic is warming (Spence et al., 2017). Tides can more effectively transfer heat to polynyas through mixing. Meanwhile, studies have shown that the sea ice in Antarctica is facing great changes (Thompson, 2022). These all mean that tides will play an increasingly important role in the study of polynyas in the future.

5 Conclusions

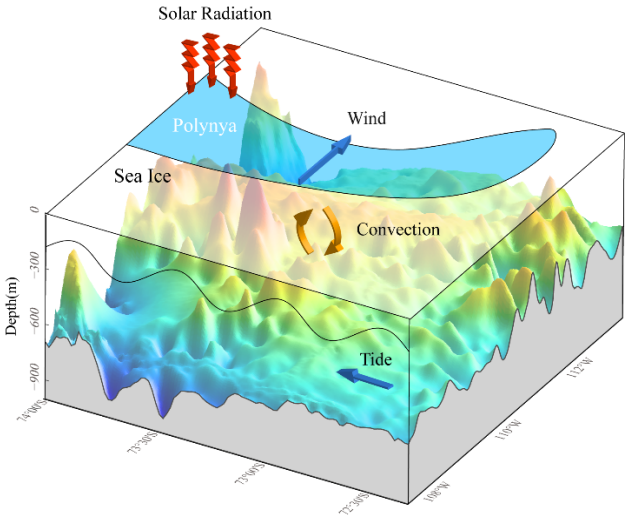

Figure 10. Schematic diagram of the formation and development of the Amundsen Sea Polynya.

This study focused on the polynya events and the change in the area of the Amundsen Sea Polynya from 2002 to 2020. According to the results, we summarized the influence of oceanic and atmospheric factors on the formation and development of the Amundsen Sea Polynya (Figure 10).The geographical location and shape of the Amundsen Sea Polynya were closely related to the topography, mostly in crescent. The Amundsen Sea Polynya began on Bear Peninsula and extended along the terrain of Bear Ridge to the open ocean. The "trigger" of the Amundsen Sea Polynya events is wind, which is the key factor in the formation of the polynya. The formation of the polynya is related to the synoptic scale wind field. The characteristics of the wind field before and after the formation of the polynya were very different. The wind during the formation of the polynya was mainly cross-ridge and observed to be perpendicular to the terrain of Bear Ridge in the Southeast (ESE and E) and Northwest (W and WNW).

Further more, this study found that the tides play a significant role in the formation of the polynyas. The present study shows that four of the five extreme events with the largest area of the Polynya may be tide-dominated. The fifth extreme event was atmosphere-dominated, caused by significant cross-ridge winds and surface net solar radiations. This shows that tides can generally provide favorable conditions for the development of the polynya, particularly for large-scale events, which has not been accounted for in most studies for polynya in Antarctica. Due to the effect of tides, the vertical convection and mixing of seawater are strengthened. The warmer seawater in the interior of the ocean is conducive to the formation and development of polynyas. Tides was the main energy source for the enhanced dissipation along the continental slopes, which was correlated with the tidal energy dissipation rate (Rippeth et al., 2015). Rough topography can influence the mixing of seawater. In addition, the interaction between tides and rough topography affects the rate of mixing. With the impact of global warming, the increase of heat transport from the atmosphere to the ocean, the decrease of sea ice, and the enhancement of mixing caused by tides need more attention.

Acknowledgments

This work is supported by the National Natural Science Foundation of China (41830538,), National Key R&D Program of China (2018YFA0605704), and the Chinese Academy of

Sciences (133244KYSB20190031, 183311KYSB20200015, and SCSIO202201).

References

Arrigo, K. R., Lowry, K. E., & van Dijken, G. L. (2012). Annual changes in sea ice and phytoplankton in polynyas of the Amundsen Sea, Antarctica. *Deep Sea Research Part II: Topical Studies in Oceanography*, 71-76, 5-15. http://doi.org/10.1016/j.dsr2.2012.03.006

Bagriantsev, N. V., Gordon, A. L., & Huber, B. A. (1989). Weddell Gyre: Temperature maximum stratum. *Journal of Geophysical Research*, 94(C6), 8331. http://doi.org/10.1029/JC094iC06p08331

Comiso, J. C., Kwok, R., Martin, S., & Gordon, A. L. (2011). Variability and trends in sea ice extent and ice production in the Ross Sea. *Journal of Geophysical Research*, 116(C4) http://doi.org/10.1029/2010JC006391

Egbert, G. D., & Erofeeva, S. Y. (2002). Efficient Inverse Modeling of Barotropic Ocean Tides. *JOURNAL OF ATMOSPHERIC AND OCEANIC TECHNOLOGY*, 19(2), 183-204. http://doi.org/10.1175/1520-0426(2002)019<0183:EIMOBO>2.0.CO;2

Gordon, A. L., & Huber, B. A. (1990). Southern ocean winter mixed layer. *Journal of Geophysical Research*, 95, 11655-11672.

Hannah, C. G., Dupont, F., & Dunphy, M. (2009). Polynyas and Tidal Currents in the Canadian Arctic Archipelago. *ARCTIC*, 62(1), 83-95. http://doi.org/10.14430/arctic115

Hausmann, U., Sallée, J. B., Jourdain, N. C., Mathiot, P., Rousset, C., Madec, G., Deshayes, J., & Hattermann, T. (2020). The Role of Tides in Ocean‐Ice Shelf Interactions in the Southwestern Weddell Sea. *Journal of Geophysical Research: Oceans*, 125(6) http://doi.org/10.1029/2019JC015847

Hellmer, H. H., Kauker, F., Timmermann, R., Determann, J., & Rae, J. (2012). Twenty-first-

505 century warming of a large Antarctic ice-shelf cavity by a redirected coastal current.
506 *NATURE*, 485(7397), 225-228. http://doi.org/10.1038/nature11064
507 Hogan, K. A., Larter, R. D., Graham, A. G. C., Arthern, R., Kirkham, J. D., Totten Minzoni, R.,
508 Jordan, T. A., Clark, R., Fitzgerald, V., Wåhlin, A. K., Anderson, J. B., Hillenbrand, C.,
509 Nitsche, F. O., Simkins, L., Smith, J. A., Gohl, K., Arndt, J. E., Hong, J., & Wellner, J.
510 (2020). Revealing the former bed of Thwaites Glacier using sea-floor bathymetry:
511 implications for warm-water routing and bed controls on ice flow and buttressing. *The*
512 *Cryosphere*, 14(9), 2883-2908. http://doi.org/10.5194/tc-14-2883-2020
513 Huot, P., Fichefet, T., Jourdain, N. C., Mathiot, P., Rousset, C., Kittel, C., & Fettweis, X. (2021).
514 Influence of ocean tides and ice shelves on ocean‐ice interactions and dense shelf water
515 formation in the D'Urville Sea, Antarctica. *OCEAN MODELLING*, 162, 101794.
516 http://doi.org/10.1016/j.ocemod.2021.101794
517 Jacobs, S., Jenkins, A., Hellmer, H., Giulivi, C., Nitsche, F., Huber, B., & Guerrero, R. (2012).
518 The Amundsen Sea and the Antarctic Ice Sheet. *OCEANOGRAPHY*, 25(3), 154-163.
519 http://doi.org/ http://dx.doi.org/10.5670/oceanog.2012.90
520 Jourdain, N. C., Molines, J., Le Sommer, J., Mathiot, P., Chanut, J., de Lavergne, C., & Madec,
521 G. (2019). Simulating or prescribing the influence of tides on the Amundsen Sea ice shelves.
522 *OCEAN MODELLING*, 133, 44-55.
523 http://doi.org/https://doi.org/10.1016/j.ocemod.2018.11.001
524 Kim, S., Lim, D., Rebolledo, L., Park, T., Esper, O., Muñoz, P., La, H. S., Kim, T. W., & Lee, S.
525 (2021). A 350-year multiproxy record of climate-driven environmental shifts in the
526 Amundsen Sea Polynya, Antarctica. *GLOBAL AND PLANETARY CHANGE*, 205, 103589.
527 http://doi.org/10.1016/j.gloplacha.2021.103589

Lee, Y. C., Park, M. O., Jung, J., Yang, E. J., & Lee, S. H. (2016). Taxonomic variability of phytoplankton and relationship with production of CDOM in the polynya of the Amundsen Sea, Antarctica. *Deep Sea Research Part II: Topical Studies in Oceanography*, 123, 30-41. http://doi.org/10.1016/j.dsr2.2015.09.002

Macdonald, G. J., Ackley, S. F., & Mestas-Nuñez, A. M. (2021). Evolution of the Amundsen Sea Polynya, Antarctica, 2016-2021. *The Cryosphere Discussions*(2021), 1-33. http://doi.org/10.5194/tc-2021-250

Markus, T., & Burns, B. A. (1993). Detection of coastal polynyas with passive microwave data. *ANNALS OF GLACIOLOGY*, 17, 351-355.

Martin, S. (2004). Okhotsk Sea Kashevarov Bank polynya: Its dependence on diurnal and fortnightly tides and its initial formation. *Journal of Geophysical Research*, 109(C9) http://doi.org/10.1029/2003JC002215

Massom, R. A., Harris, P. T., Michael, K. J., & Potter, M. J. (1998). The distribution and formative processes of latent-heat polynyas in East Antarctica. In W. F. Budd (Ed.), *ANNALS OF GLACIOLOGY* (27, pp. 420-426). (Reprinted.

Meehl, G. A., Arblaster, J. M., Chung, C. T. Y., Holland, M. M., DuVivier, A., Thompson, L., Yang, D., & Bitz, C. M. (2019). Sustained ocean changes contributed to sudden Antarctic sea ice retreat in late 2016. *Nature Communications*, 10(1) http://doi.org/10.1038/s41467-018-07865-9

Melling, H., Lake, R. A., Topham, D. R., & Fissel, D. B. (1984). Oceanic thermal structure in the western Canadian Arctic. *CONTINENTAL SHELF RESEARCH*, 3(3)

Morales Maqueda, M. A., Willmott, A. J., & Biggs, N. R. T. (2004). Polynya dynamics; a review of observations and modeling. *Reviews of geophysics (1985)*, 42(1), G1001-G1004.

http://doi.org/10.1029/2002RG000116

Nakayama, Y., Cilan, C., & Seroussi, H. (2021). Impact of subglacial freshwater discharge on Pine Island ice shelf. *GEOPHYSICAL RESEARCH LETTERS*, 48(18) http://doi.org/10.1029/2021GL093923

Nitsche, F. O., Jacobs, S. S., Larter, R. D., & Gohl, K. (2007). Bathymetry of the Amundsen Sea continental shelf: Implications for geology, oceanography, and glaciology. *Geochemistry, Geophysics, Geosystems*, 8(10), n/a-n/a. http://doi.org/10.1029/2007GC001694

Ou, H. W. (1991). Some effects of a seamount on oceanic flows. *JOURNAL OF PHYSICAL OCEANOGRAPHY*, 21(12), 1835-1845. http://doi.org/10.1175/1520-0485(1991)021<1835:SEOASO>2.0.CO;2

Parkinson, C. L. (1983). On the Development and Cause of the Weddell Polynya in a Sea Ice Simulation. *JOURNAL OF PHYSICAL OCEANOGRAPHY*, 13(3), 501-511. http://doi.org/10.1175/1520-0485(1983)013<0501:OTDACO>2.0.CO;2

Penwarden, A. D. (1973). Acceptable wind speeds in towns. *Building Science*, 8(3), 259-267.

Preusser, A., Ohshima, K. I., Iwamoto, K., Willmes, S., & Heinemann, G. (2019). Retrieval of Wintertime Sea Ice Production in Arctic Polynyas Using Thermal Infrared and Passive Microwave Remote Sensing Data. *JOURNAL OF GEOPHYSICAL RESEARCH-OCEANS*, 124(8), 5503-5528. http://doi.org/10.1029/2019JC014976

Richter, O., Gwyther, D. E., King, M. A., & Galton-Fenzi, B. K. (2022). The impact of tides on Antarctic ice shelf melting. *The Cryosphere*, 16(4), 1409-1429. http://doi.org/10.5194/tc-16-1409-2022

Rignot, E., Mouginot, J., Scheuchl, B., van den Broeke, M., van Wessem, M. J., & Morlighem, M. (2019). Four decades of Antarctic Ice Sheet mass balance from 1979 – 2017.

574 *Proceedings of the National Academy of Sciences*, 116(4), 1095-1103.
575 http://doi.org/10.1073/pnas.1812883116
576 Rippeth, T. P., Lincoln, B. J., Lenn, Y., Green, J. A. M., Sundfjord, A., & Bacon, S. (2015).
577 Tide-mediated warming of Arctic halocline by Atlantic heat fluxes over rough topography.
578 *Nature Geoscience*, 8(3), 191-194. http://doi.org/10.1038/ngeo2350
579 Schlosser, E., Haumann, F. A., & Raphael, M. N. (2018). Atmospheric influences on the
580 anomalous 2016 Antarctic sea ice decay. *The Cryosphere*, 12(3), 1103-1119.
581 http://doi.org/10.5194/tc-12-1103-2018
582 Shepherd, A., Gilbert, L., Muir, A. S., Konrad, H., McMillan, M., Slater, T., Briggs, K. H.,
583 Sundal, A. V., Hogg, A. E., & Engdahl, M. E. (2019). Trends in Antarctic Ice Sheet
584 Elevation and Mass. *GEOPHYSICAL RESEARCH LETTERS*, 46(14), 8174-8183.
585 http://doi.org/10.1029/2019GL082182
586 Shepherd, A., & Wingham, D. (2007). Recent sea-level contributions of the Antarctic and
587 Greenland ice sheets [Journal Article]. *SCIENCE*, 315(5818), 1529-1532.
588 http://doi.org/10.1126/science.1136776
589 Spence, P., Holmes, R. M., Hogg, A. M., Griffies, S. M., Stewart, K. D., & England, M. H.
590 (2017). Localized rapid warming of West Antarctic subsurface waters by remote winds.
591 *Nature Climate Change*, 7(8), 595-603. http://doi.org/10.1038/nclimate3335
592 Spreen, G., Kaleschke, L., & Heygster, G. (2008). Sea ice remote sensing using AMSR-E 89-
593 GHz channels. *Journal of Geophysical Research*, 113(C2)
594 http://doi.org/10.1029/2005JC003384
595 Stammerjohn, S., Massom, R., Rind, D., & Martinson, D. (2012). Regions of rapid sea ice
596 change: An inter-hemispheric seasonal comparison. *GEOPHYSICAL RESEARCH*

LETTERS, 39(6), n/a-n/a. http://doi.org/10.1029/2012GL050874

Thompson, T. (2022). Antarctic sea ice hits lowest minimum on record. *NATURE* http://doi.org/10.1038/d41586-022-00550-4

Thuróczy, C., Alderkamp, A., Laan, P., Gerringa, L. J. A., Mills, M. M., Van Dijken, G. L., De Baar, H. J. W., & Arrigo, K. R. (2012). Key role of organic complexation of iron in sustaining phytoplankton blooms in the Pine Island and Amundsen Polynyas (Southern Ocean). *Deep Sea Research Part II: Topical Studies in Oceanography*, 71-76, 49-60. http://doi.org/10.1016/j.dsr2.2012.03.009

Tozer, B., Sandwell, D. T., Smith, W. H. F., Olson, C., Beale, J. R., & Wessel, P. (2019). Global Bathymetry and Topography at 15 Arc Sec: SRTM15+. *Earth and Space Science*, 6(10), 1847-1864. http://doi.org/10.1029/2019EA000658

Vincent, R. F., & Marsden, R. F. (2008). A Study of Tidal Influences in the North Water Polynya Using Short Time Span Satellite Imagery. *ARCTIC*, 61(4), 373-380. http://doi.org/10.14430/arctic45

Wessel, P., Luis, J. F., Uieda, L., Scharroo, R., Wobbe, F., Smith, W. H. F., & Tian, D. (2019). The Generic Mapping Tools Version 6. *Geochemistry, Geophysics, Geosystems*, 20(11), 5556-5564. http://doi.org/10.1029/2019GC008515

Zhang, Y., Zhang, Y., Xu, D., Chen, C., Shen, X., Hu, S., Chang, L., Zhou, X., & Feng, G. (2021). Impacts of atmospheric and oceanic factors on monthly and interannual variations of polynya in the East Siberian Sea and Chukchi Sea. *Advances in Climate Change Research*, 12(4), 527-538. http://doi.org/10.1016/j.accre.2021.07.005